2004

Distinct roles for the AAA ATPases NSF and p97 in the secretory pathway

Seema Dalal
Washington University School of Medicine in St. Louis

Meredith F.N. Rosser
University of North Carolina at Chapel Hill

Douglas M. Cyr
University of North Carolina at Chapel Hill

Phyllis I. Hanson
Washington University School of Medicine in St. Louis

Molecular Biology of the Cell
Vol. 15, 637–648, February 2004

Distinct Roles for the AAA ATPases NSF and p97 in the Secretory Pathway

Seema Dalal,* Meredith F. N. Rosser,† Douglas M. Cyr,† and Phyllis I. Hanson*‡

*Washington University School of Medicine, Department of Cell Biology and Physiology, St. Louis, Missouri 63110; and †University of North Carolina, Department of Cell and Developmental Biology, Chapel Hill, North Carolina 27599

Submitted February 21, 2003; Revised October 17, 2003; Accepted October 20, 2003
Monitoring Editor: Benjamin Glick

NSF and p97 are related AAA proteins implicated in membrane trafficking and organelle biogenesis. p97 is also involved in pathways that lead to ubiquitin-dependent proteolysis, including ER-associated degradation (ERAD). In this study, we have used dominant interfering ATP-hydrolysis deficient mutants (NSF(E329Q) and p97(E578Q)) to compare the function of these AAA proteins in the secretory pathway of mammalian cells. Expressing NSF(E329Q) promotes disassembly of Golgi stacks into dispersed vesicular structures. It also rapidly inhibits glycosaminoglycan sulfation, reflecting disruption of intra-Golgi transport. In contrast, expressing p97(E578Q) does not affect Golgi structure or function; glycosaminoglycans are normally sulfated and secreted, as is the VSV-G ts045 protein. Instead, expression of p97(E578Q) causes ubiquitinated proteins to accumulate on ER membranes and slows degradation of the ERAD substrate cystic-fibrosis transmembrane-conductance regulator. In addition, expression of p97(E578Q) eventually causes the ER to swell. More specific assessment of effects of p97(E578Q) on organelle assembly shows that the Golgi apparatus disperses and reassembles normally after treatment with brefeldin A and during mitosis. These findings demonstrate that ATP-hydrolysis–dependent activities of NSF and p97 in the cell are not equivalent and suggest that only NSF is directly involved in regulating membrane fusion.

INTRODUCTION

Membrane fusion is an essential step in all forms of vesicle trafficking and organelle assembly. Fusion is driven by a series of regulated protein–protein interactions. Many participating proteins have been identified, and their specific roles are gradually coming to light (reviewed in Jahn *et al.*, 2003). Among these proteins are a number of ATPases.

N-ethyl maleimide sensitive factor (NSF) was one of the first proteins specifically linked to membrane fusion (Wilson *et al.*, 1989). It belongs to a family of chaperone-like ATPases known as AAA (ATPases associated with a variety of cellular activities) proteins (Neuwald *et al.*, 1999). NSF together with α-SNAP (soluble NSF attachment protein) dissociates the SNARE (SNAP receptor) complexes that promote association and fusion of cellular membranes. More recently, NSF has also been implicated in other cellular processes on the basis of its ability to bind the AMPA receptor GluR2, β-arrestin 1, and GATE-16 (reviewed in Whiteheart *et al.*, 2001). However, its role in SNARE disassembly and membrane fusion remains its best understood function.

Not all ATP-requiring steps that lead to membrane fusion can be attributed to NSF (Goda and Pfeffer, 1991; Latterich and Schekman, 1994; Rodriguez *et al.*, 1994; Wilson, 1995). Other ATPases must therefore be involved. One AAA protein thought to be an alternate to NSF is known as p97 (also referred to as valosin-containing protein, VCP). p97 is an abundant and highly conserved protein (Peters *et al.*, 1990) whose cellular function has been the subject of much debate. A break in the mystery of p97's function came when it turned up as a factor involved in NSF-independent in vitro fusion between membranes of the ER (Latterich *et al.*, 1995), mitotic Golgi fragments (Rabouille *et al.*, 1995), ilimaquinone-generated Golgi fragments (Acharya *et al.*, 1995), low-density microsomes (Roy *et al.*, 2000), and fragments of the nuclear envelope (Hetzer *et al.*, 2001). The additional finding that p97 could bind to syntaxin 5 in vitro (Rabouille *et al.*, 1998) led to the proposal that p97 might carry out a reaction similar to the SNARE complex disassembly mediated by NSF, but on different SNAREs (Patel *et al.*, 1998; Rabouille *et al.*, 1998). However, although p97 has been shown to release the t-SNARE syntaxin 5 from a complex with p47 and VCIP135 (Uchiyama *et al.*, 2002), it has so far not been found to disassemble complexes consisting of multiple SNARE proteins. Therefore the mechanism by which p97 participates in in vitro fusion reactions remains unknown.

Meanwhile, a variety of seemingly unrelated activities of p97 have emerged. These include roles in ubiquitin- and proteasome-dependent degradation of cytosolic proteins (Ghislain *et al.*, 1996; Dai *et al.*, 1998; Dai and Li, 2001), ER-associated degradation (ERAD; reviewed in Bays and Hampton, 2002; Tsai *et al.*, 2002), and regulated ubiquitin-dependent processing (Rape *et al.*, 2001). It is believed that different adaptor proteins direct p97 to perform these varied cellular activities. These adaptors include p47 (Kondo *et al.*,

Article published online ahead of print. Mol. Biol. Cell 10.1091/mbc.E03–02–0097. Article and publication date are available at www.molbiolcell.org/cgi/doi/10.1091/mbc.E03–02–0097.

‡ Corresponding author. E-mail address: phanson@cellbiology.wustl.edu.

Abbreviations used: AAA, ATPases associated with a variety of cellular activities; α-SNAP, soluble NSF attachment protein; GAGs, glycosaminoglycans; SNARE, SNAP receptor.

1997), Ufd1/Npl4 (Meyer *et al.*, 2000, 2002), VCIP135 (Uchiyama *et al.*, 2002), and SVIP (Nagahama *et al.*, 2003).

Although the mechanism by which AAA ATPases such as NSF and p97 use ATP to modulate the structure of their substrates is not known, the overall homology between these two enzymes makes the idea that they might operate by a similar mechanism attractive. Each consists of an N domain and two adjacent AAA domains referred to as D1 and D2. The homologous N domains are attached by flexible linkers to hexameric rings formed by the AAA domains and are important in allowing the enzymes to bind their intended substrates (Nagiec *et al.*, 1995; Dai and Li, 2001; Yuan *et al.*, 2001). Conformational changes take place in both enzymes coincident with the ATP-hydrolysis cycle (Hanson *et al.*, 1997; Rouiller *et al.*, 2000, 2002; Beuron *et al.*, 2003) and are presumably transmitted to bound substrate proteins, resulting in their modification.

To compare the functions of p97 and NSF in the secretory pathway, we looked at the effects of expressing dominant interfering mutants of these enzymes in mammalian cells. We find that each mutant inhibits distinct and nonoverlapping cellular processes. Our results support a direct role for NSF in membrane fusion. More strikingly, they suggest a different mode of action for p97 in which its primary role is in the handling of ubiquitinated proteins.

MATERIALS AND METHODS

Cloning and DNA Manipulation

For mammalian expression of NSF and NSF(E329Q) GFP fusions, Chinese hamster ovary NSF and NSF(E329Q) were PCR-amplified and cloned between *Xho*I and *Bam*HI sites in EGFPN1 (Clontech, Palo Alto, CA). This resulted in a C-terminal GFP fusion with a linker of VDPPVAT between the last residue of NSF (K) and the first residue of GFP. Tetracycline-regulated plasmids were made as follows: NSF-GFP fusion constructs were excised from EGFPN1 using *Xho*I and *Xba*I and subcloned into pcDNA4/TO (Invitrogen, San Diego, CA). NSF and NSF(E329Q) myc constructs were created by subcloning from the NSF pcDNA4/TO constructs using *Bam*HI to excise the NSF. This was introduced into the *Bam*HI site of pcDNA4/TO myc/HisC resulting in a C-terminal myc/His fusion and a linker sequence of SDPLVQCGGILQISSTVAAARA between NSF and myc.

A mammalian expression construct for p97 was made by PCR amplification from mouse p97 DNA and cloning between *Bam*HI and *Not*I in pcDNA3.1 myc/HisB (Invitrogen). This results in a C-terminal myc fusion with a linker sequence of GGRSSLEGPRF between the last amino acid of p97 (G) and the first amino acid of the myc tag. p97 mutants (p97(E305Q), p97(E578Q), and p97(E305/578Q)) were generated by Stratagene Quickchange (La Jolla, CA) mutagenesis using the p97 pcDNA3.1 myc/HisB vector as DNA template in the reactions. These p97 variants were then subcloned into the tetracycline-inducible vector pcDNA4/TO myc/HisB between the restriction sites *Bam*HI and *Age*I, resulting in a C-terminal myc/His tag and a linker that is identical to that in the p97 pcDNA3.1 myc/HisB vector.

For bacterial protein expression, p97 was PCR-amplified and cloned between the *Bam*HI and *Not*I restriction sites in pet28a (Novagen, Madison, WI), resulting in a construct with a N-terminal His tag followed by thrombin cleavage site, a T7 tag and a amino acid linker (RGS) before the initial M of p97. p97(E305Q), p97(E578Q), and p97(E305/578Q) were generated by Stratagene Quickchange mutagenesis from the p97 pet28a construct. The sequences of all constructs were verified by nucleotide sequencing.

Expression and Purification of Recombinant p97

Proteins were expressed in BL21(DE3) at room temperature by induction with 0.4 mM IPTG at an $OD_{600\ nm}$ of ~1.2. Cells were harvested 4 h after induction. Proteins were purified essentially as described (Meyer *et al.*, 2000). After elution with imidazole, fractions containing p97 were pooled and concentrated in a Vivaspin concentrator (Vivascience, Hanover, Germany). They were further purified on a Superdex 200 HR 10/30 gel filtration column (Amersham Biosciences, Piscataway, NJ) in gel filtration buffer (50 mM HEPES, 150 mM KCl, 1 mM β-mercaptoethanol, 2 mM $MgCl_2$, 5% glycerol, 0.5 mM ATP, pH 7.4). Peak protein fractions were snap-frozen in liquid nitrogen. Protein concentrations were determined by Bradford assay using bovine serum albumin (BSA) as a standard (Bio-Rad, Cambridge, MA). Quick-freeze deep-etch EM of the p97 molecules was performed as described (Hanson *et al.*, 1997).

ATPase Activity Assay

ATPase activities of p97, p97(E305Q), p97(E578Q), and p97(E305/578Q) were assayed at 37°C in assay buffer containing 25 mM HEPES, 0.5 mM dithiothreitol (DTT), 100 mM NaCl, 10% glycerol, 10 mM $MgCl_2$, pH 7.6, and 2 mM ATP. Aliquots removed at 0, 15, 30, 45, and 60 min were quenched in 50 mM EDTA on ice. Released phosphate was detected using a colorimetric assay as described (Lill *et al.*, 1990).

Generation of Cell Lines and Cell Culture Techniques

U2OS TRex cells stably transfected with a tetracycline repressor plasmid (Invitrogen) were transfected to generate cell lines expressing NSF and p97. Medium containing 50 μg/ml hygromycin B (Invitrogen) and 125 μg/ml zeocin (Invitrogen) was added to select the stable cell lines. Approximately 12 d later, colonies of zeocin-resistant cells appeared. On average 25–30 colonies for each desired cell line were transferred into separate wells and screened. In the case of NSF(E329Q), 50 colonies were screened. Immunofluorescence and Western blot analysis were used to identify lines that expressed protein only in the presence of tetracycline. Cells were maintained with 50 μg/ml hygromycin B and 65 μg/ml zeocin. Protein expression was induced by the addition of 1 μg/ml tetracyline for the indicated times. At the standard times used for experiments (12 h for p97 cell lines and 5.5 h for NSF cell lines), 80–90% of the cells expressed the exogenous, tagged protein.

Immunofluorescence, Immunoprecipitation, and Western Blots

Immunofluorescence was performed on cells fixed in 4% paraformaldehyde/4% sucrose and permeabilized with 0.1% Triton X-100 with the exception of those cells stained with anti-β-COP which were permeabilized with a mixture of 0.1% Triton X-100/0.05% SDS. For saponin (Sigma, St. Louis, MO) treatment of cells, coverslips were briefly (~5 s) exposed to 0.05% saponin/phosphate-buffered saline/4% sucrose before fixation.

Immunoprecipitations were carried out with cells solubilized in 0.5% Triton X-100 under ATP-hydrolyzing conditions (30 mM HEPES, 100 mM NaCl, 5 mM $MgCl_2$, 2 mM ATP, 1 mM DTT, EDTA-free protease inhibitors, pH 7.4). 9E10 anti-myc ascites or affinity-purified polyclonal anti-GFP antibodies (B5) were used and collected with protein G-Sepharose beads (Amersham). Immunoblots were developed as described (Hanson *et al.*, 1997).

The following antibodies were used in this study: Mouse monoclonal anti-p97 (Research Diagnostics, Flanders, NJ), rabbit anti-myc (Cell Signaling Technology, Beverly, MA), rabbit anti-giantin (Covance, Richmond, CA), mouse monoclonal anti-PDI and rabbit anti-calnexin (SPA-860; Stressgen, Victoria, BC, Canada), mouse monoclonal ubiquitin FK2 (Affiniti Research Products, Exeter, UK), mouse monoclonal anti–α-tubulin (clone DM 1A) and anti-β-COP (clone maD; Sigma), rabbit anti-COPII (Affinity Bioreagents Inc., Golden, CO), rabbit polyclonal (B1) and mouse monoclonal anti-NSF (Cl83.11, gift from Reinhard Jahn), mouse monoclonal anti–α-SNAP (Cl77.2, available from Synaptic Systems, Göttingen, Germany), mouse monoclonal anti-myc (9E10), rabbit anti-GFP (B5), rabbit anti-p47 (gift from Graham Warren), mouse monoclonal anti-p115 (BD Transduction Labs, Lexington, KY), sheep anti-TGN46 (Serotec, Oxford, UK). Secondary goat anti-mouse, goat anti-rabbit, and donkey anti-sheep antibodies conjugated to Alexa 488 or Alexa 568 were purchased from Molecular Probes (Eugene, OR).

CFTR Degradation

p97(E578Q) cells were grown in six-well trays and infected with 1.2×10^9 adenoviral particles containing a ΔF508 CFTR expression vector (provided by the Vector Core of the Institute for Human Gene Therapy at the University of Pennsylvania School of Medicine, Philadelphia, PA). Thirty-six hours after infection, tetracycline was either added (ON) or not (OFF). Twelve hours after induction, cells were starved in methionine-free media for 45 min, and then labeled with 100 μCi *trans*-^{35}S-label (ICN, Costa Mesa, CA) per well for 30 min. After labeling, cells were washed and incubated in media containing 25 μg/ml cycloheximide for the indicated chase times. Cells were solubilized in 700 μl of RIPA buffer (150 mM NaCl, 50 mM HEPES, pH 7.4, 1% NP-40, 0.5% deoxycholate, 0.2% SDS, 0.2% BSA, 0.5 mM phenylmethylsulfonyl fluoride) with EDTA-free protease inhibitor (Roche, Nutley, NJ) for 30 min at 4°C. To preclear the cell lysates, they were incubated with 30 μl of a 50% slurry of Pansorbin cells (Calbiochem, La Jolla, CA) at 4°C. Pansorbin cells and insoluble material were removed by centrifugation at 10,000 rpm for 10 min. Immunoprecipitation of the ΔF508 CFTR was carried out with 5 μl of polyclonal antisera raised against the N-terminus of CFTR (Meacham *et al.*, 1999). Immunoprecipitated material was eluted from the beads by heating at 37°C for 15 min in 2× SDS sample buffer. Eluted material was analyzed by SDS-PAGE and fluorography. Densitometry was carried out on a Bio-Rad GS-700 densitometer.

GAG Sulfation Assay

To monitor sulfated GAG synthesis, we measured ^{35}S-labeled sulfated GAGs as follows (based on Miller and Moore, 1992). Cells were incubated in 5 mM xyloside (4-methylumbelliferyl-β-D-xyloside, Sigma), for 30 min to initiate

GAG synthesis, and then labeled with 200 μCi/ml ^{35}S-sulfate in DME/HEPES at 37°C for 2 min. Reactions were terminated by adding wash solution containing 4 mM unlabeled Na_2SO_4. Cells were lysed in KHMgE (70 mM KCl, 30 mM HEPES, 5 mM $MgCl_2$, 3 mM EGTA, pH 7.4) containing 1% Triton. Samples were digested with pronase E (Sigma) for 1 h and then precipitated with 15% cetylpyridinium chloride (Sigma) and chondroitin sulfate (Sigma) for 1 h. Samples were collected on nitrocellulose filters and counted in scintillation fluid.

Secretion of ^{35}S-labeled sulfated GAGs was measured by labeling sulfated GAGs for 2 min with ^{35}S-sulfate as above, and then chasing in DME/HEPES at 37°C for 0, 5, 10, 15, and 20 min. ^{35}S-labeled sulfated GAGs were then collected separately from the cell media and the lysed cells as above. The results of all experiments shown were confirmed in three independent trials.

VSV-G ts045 Trafficking

p97(E578Q) and U2OS cells were transfected with VSV-G ts045-GFP (Presley *et al.*, 1997) using Lipofectamine (Invitrogen) according to the manufacturer's instructions. After transfection, cells were shifted to 38.5°C. Four hours later, tetracycline was added and coverslips were incubated at 38.5°C for an additional 12 h. Cycloheximide (100 μg/ml) was then added for 30 min before moving the coverslips to 32°C. Coverslips were removed, fixed, and processed for immunofluorescence at 0, 30, 60, and 120 min later, as described above, using rabbit anti-GFP antibody.

Brefeldin A Treatment of Cells

Cells were incubated in 5 μg/ml brefeldin A (BFA; Molecular Probes) in media at 37°C. After 40 min, coverslips were either fixed directly or allowed to recover for 2 h and then fixed.

Electron Microscopy

For traditional thin sections, cells grown to ~70% confluence in a 35-mm dish were treated with tetracycline, washed in phosphate-buffered saline, fixed in 2.5% gluteraldehyde in Na-cacodylate in situ, embedded, sectioned, and stained with uranyl acetate according to standard procedures. For freeze-substitution, cells were grown and induced on 4 × 4-mm glass coverslips. Coverslips were rapidly frozen and transferred to liquid nitrogen (Heuser *et al.*, 1979). Freeze-substitution was performed by exposing the coverslip to frozen 4% osmium tetroxide in anhydrous acetone (Heuser and Reese, 1981). Araldite-embedded samples were removed from the coverslip and cut into thin sections. Thin sections were viewed in a JEOL transmission EM operating at 100 kV (Peabody, MA).

Light Microscopy

Confocal microscopy was performed on a Radiance 2000 Bio-Rad microscope using 488- and 543-nm laser lines. All images were acquired with sequential scans using LaserSharp 2000. Images were prepared using Adobe Photoshop (Adobe Systems, San Jose, CA).

RESULTS

Inverse Arrangement of AAA Domains in NSF and p97

NSF and p97 share a common domain structure, consisting of N domains followed by two AAA domains referred to as D1 and D2. Previously, it has been shown that the D1 domain is responsible for NSF's ATPase activity (Whiteheart *et al.*, 1994). In contrast, NSF's D2 domain stabilizes the hexameric state of the enzyme but does not hydrolyze ATP (Nagiec *et al.*, 1995).

In the case of p97, it was not clear at the start of this study which (or both) of the two AAA domains is directly responsible for the enzyme's ATPase activity. Both of p97's AAA domains are more homologous to each other and the D1 domain of NSF than to NSF's D2 domain. There are precedents in other two domain AAA proteins for D1, D2, or both being critical for function (Vale, 2000).

To define the relative contributions of the AAA domains to p97's ATPase activity, we mutated residues in each that are known to be important for function in related ATPases. The second acidic residue in each Walker B DExx motif was replaced with a glutamine to generate potential hydrolysis defective mutants (Hung *et al.*, 1998). We created three p97 variants (p97(E305Q), p97(E578Q), and p97(E305/578Q)) and purified them after expression in *Escherichia coli*. All assembled into oligomers that eluted from a size exclusion column at a position consistent with a 540-kDa hexamer (our unpublished observations). Deep-etch electron microscopy confirmed that all variants assembled into cylinders indistinguishable from those formed by wild-type p97 (Figure 1A).

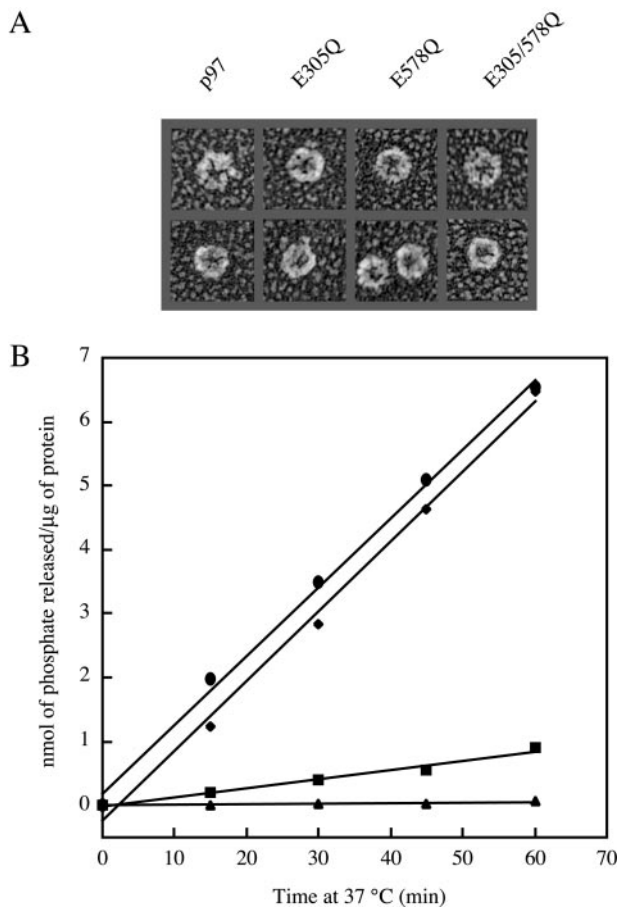

Figure 1. The D2 domain of p97 is its dominant ATPase domain. (A) Deep-etch electron microscopy of bacterially expressed and purified p97 demonstrates that Walker B DExx box mutations in D1(p97(E305Q)), D2 (p97(E578Q)), or both (p97(E305/578Q)) do not alter its normal hexameric cylindrical structure. Molecules are 13–15 nm in diameter. (B) Normal ATPase activity of wtp97 (♦) and p97(E305Q) (●) versus diminished ATPase activity in p97(E578Q) (■) and p97(E305/578Q) (▲) indicates that its D2 domain is responsible for the majority of the enzyme's ATPase activity. Data shown are an average of two independent measurements and are representative of four independent trials.

Measurements of ATP hydrolysis by wild-type and the mutants revealed differences in their ability to hydrolyze ATP (Figure 1B). p97(E305Q) was similar to wild-type p97 and hydrolyzed ATP at a rate comparable to that previously reported for p97/VCP (~7 nmol/h/μg p97; Peters *et al.*, 1992; Egerton and Samelson, 1994; Meyer *et al.*, 1998), whereas p97(E578Q) had severely impaired ATPase activity. The double mutant p97(E305/578Q) had no ATPase activity. These data show that the D2 domain of p97 is responsible for most of the enzyme's ATPase activity and are consistent with data recently reported by others (Lamb *et al.*, 2001; Kobayashi *et al.*, 2002; Song *et al.*, 2003; Ye *et al.*, 2003). The dominance of the D2 domain in p97 contrasts with that of the D1 domain in NSF, indicating that the N-domains of the respective enzymes must be coupled to their hydrolytically

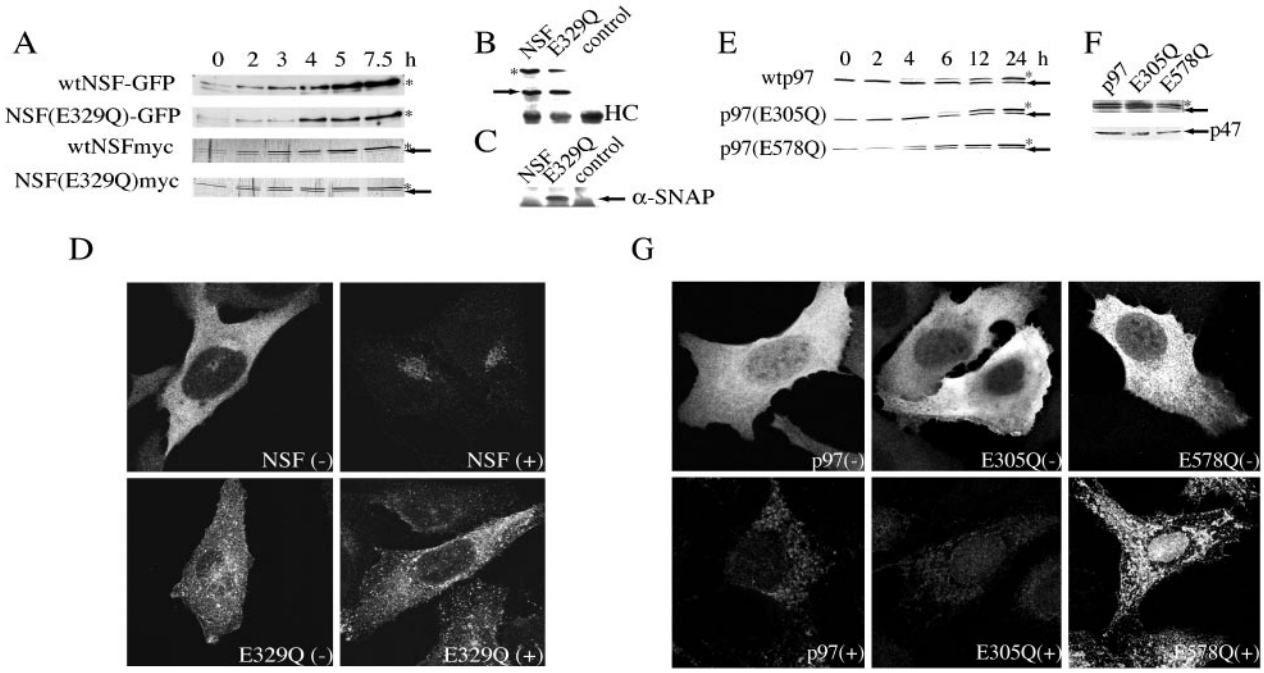

Figure 2. Properties of U2OS cell lines expressing NSF and p97 variants. (A) Time courses of induction of NSF-GFP versus NSFmyc in human osteosarcoma U2OS cells expressing wild-type and mutant proteins after addition of tetracycline. GFP-tagged proteins were detected with an anti-GFP antibody, and myc-tagged and endogenous NSF were seen using a monoclonal anti-NSF antibody. Tagged proteins are indicated with an asterisk, and endogenous protein is marked with an arrow. (B) Immunoprecipitation from extracts of cells expressing NSF-GFP or NSF(E329Q)-GFP with anti-GFP antibody retrieves endogenous NSF. Samples immunoprecipitated with GFP antibodies were blotted with a monoclonal antibody recognizing NSF. Control represents a GFP expressing cell line. The endogenous protein is marked with an arrow. HC is the IgG heavy chain. (C) α-SNAP immunoprecipitates with NSF(E329Q)myc in the presence of Mg^{2+}ATP and does not immunoprecipitate with NSFmyc. Control represents untransfected U2OS cells. Anti-myc antibody was used for immunoprecipitation, and samples were blotted with antibody recognizing α-SNAP. α-SNAP migrates just behind IgG light chain, seen along the bottom of the blot. (D) Intracellular distribution of NSF and NSF(E329Q) before (−) and after (+) saponin permeabilization shows retention of the mutant on intracellular membranes. Each box is 83 × 83 μm. (E) Time courses of induction of wtp97, p97(E305Q), and p97(E578Q)myc after addition of tetracycline to stably transfected cell lines. Tagged proteins are indicated with an asterisk, and endogenous protein is marked with an arrow. (F) Top panel: Immunoprecipitation with anti-myc antibody shows that endogenous p97 coassembles with induced wtp97, p97(E305Q), and p97(E578Q)myc in vivo. Precipitated proteins are stained with Ponceau Red and the identity of the bands was confirmed by immunoblotting with p97 antibodies (unpublished observations). Tagged proteins are indicated with an asterisk, and endogenous protein is marked with an arrow. Immunoblots with anti-p97 antibody of anti-myc antibody depleted p97(E578Q) lysates confirmed that a majority of the endogenous p97 coassembles with the p97(E578Q) (our unpublished observations). Bottom panel: The same immunoprecipitates blotted with an antibody against p47. (G) Intracellular distribution of wtp97, p97(E305Q), and p97(E578Q)myc before (−) and after (+) permeabilization with saponin. All images were collected at the same laser power on a confocal microscope. Each box is 83 × 83 μm.

active ATPase domains in different ways. Possible mechanisms for this are suggested by the recent structure of p97 (DeLaBarre and Brünger, 2003).

NSF and p97 Walker B Mutants Accumulate on Membranes

To compare the roles of NSF and p97 in vivo, we generated cell lines in which expression of wild-type or hydrolysis-defective mutants could be induced by adding tetracycline. Induced proteins were marked with C-terminal epitope tags, either myc (both enzymes) or GFP (NSF). Shown in Figure 2, A and E, is the time course of protein expression in each of the cell lines. p97 is more abundant than NSF in the cell (comprising ~1% of cell protein vs. ~0.1% for NSF), and thus it took longer for induced p97 to reach endogenous levels. Experiments with NSF cell lines were typically done 5.5 h after induction, whereas those with p97 cell lines were done 12 h after induction. For the NSF(E329Q) and p97(E578Q) cell lines, these times are twice as long as it takes for the mutant protein to reach a level equivalent to endogenous protein. To confirm that most or all holoenzymes contain some mutant subunits, we immunoprecipitated induced proteins and found that endogenous NSF or p97 coprecipitated with their tagged counterparts at a ratio similar to that of the proteins in the extract (Figure 2, B and F). It has previously been shown that the presence of any inactive subunits within a holoenzyme destroys NSF (Whiteheart *et al.*, 1994) and p97 (Wang *et al.*, 2003) function. Based on this and the fact that ATP-bound NSF has highest affinity for its substrates (Hanson *et al.*, 1997), we anticipated that Walker B mutations in each enzyme's active AAA domain would function as dominant inhibitors and accumulate on their respective substrates in the cell leading to effective inhibition even in the presence of endogenous enzyme.

What effect do these mutations have on protein localization? As expected, wtNSF was cytosolic and excluded from the nucleus (Figure 2D). Brief permeabilization with saponin before fixation depleted the cell of wtNSF, leaving only a small amount on the membranes of the Golgi apparatus. In contrast, NSF(E329Q) was enriched on various structures throughout the cell and was only minimally released by saponin permeabilization (Figure 2D). All known substrates

for NSF are membrane proteins (primarily the SNAREs); hence the shift of NSF(E329Q) from cytosol to membranes is consistent with binding and retention on these membrane associated substrates. Furthermore, when NSF was immunoprecipitated from detergent-solubilized cell extracts in the presence of Mg^{2+}ATP, α-SNAP coprecipitated with NSF(E329Q) but not with wtNSF (Figure 2C). This shows that normal ATP-sensitive interactions of NSF persist under hydrolyzing conditions with NSF(E329Q) and confirms that NSF(E329Q) functions as a "substrate trap."

Similar experiments with cell lines expressing p97 and its mutants showed that all variants of p97 were present in both the cytosol and nucleus, but the predicted substrate trap p97(E578Q) was selectively retained on reticular membranes after saponin permeabilization (Figure 2G). These membranes could be costained with markers of the ER (unpublished data). These experiments show that mutation of the D2 AAA domain of p97 traps a significant portion of p97 on membranes in vivo. Note that in contrast to the behavior of NSF(E329Q), there is also a sizeable pool of soluble p97(E578Q), possibly reflecting the presence of soluble substrates. Together with experiments described below, these results demonstrate that D2 is the AAA domain most critical for p97's activity in vivo as well as in vitro. The presence of p47 in immunoprecipitates of all three p97 variants confirmed that physiologically relevant interactions are maintained (Figure 2F).

NSF(E329Q) Disrupts Golgi Structure

To monitor effects of expressing NSF(E329Q) on organelle morphology, we carried out immunofluorescence using markers for a variety of cellular compartments. Induction of myc- or GFP-tagged wtNSF had no effect on the normal morphology of either the Golgi or the ER (Figure 3, A and C). In contrast, expression of myc- or GFP-tagged NSF(E329Q) disrupted the organization of the Golgi apparatus (Figure 3, B and D). Membranes containing giantin (a Golgi membrane protein) quickly dispersed throughout the cell into small and large punctate structures and then over several hours coalesced into discrete clusters concentrated near the nucleus and the microtubule organizing center. Other markers for the Golgi apparatus and the TGN, including p115, β-COP, and TGN46, were similarly dispersed in NSF(E329Q) cells (not shown). Not all NSF(E329Q) containing structures colocalized with giantin (Figure 3B), suggesting that NSF(E329Q) was also trapped on other membranes. The structure of the ER was not apparently perturbed by expression of NSF(E329Q) (Figure 3D). ER exit sites marked by the COPII coat complex were present at the usual density throughout the cell, and the nuclear envelope appeared intact (our unpublished observations).

To further define the changes caused by NSF(E329Q), we examined the ultrastructure of cells expressing wtNSF or NSF(E329Q) by thin-section electron microscopy (EM; Figure 4). U2OS cells contain well-organized and abundant Golgi stacks, with variable degrees of dilation at their rims, and these were unaffected by expression of wtNSF (Figure 4A). The ribosome studded ER and nuclear envelope in these cells were similarly typical. After induction of NSF(E329Q), likely Golgi remnants (Figure 4B) and pools of vesicles (Figure 4C) were seen in the perinuclear region normally occupied by Golgi stacks, which were now absent. These results confirm that NSF activity is needed to maintain Golgi structure and imply that it is not required for vesicle formation from Golgi stacks.

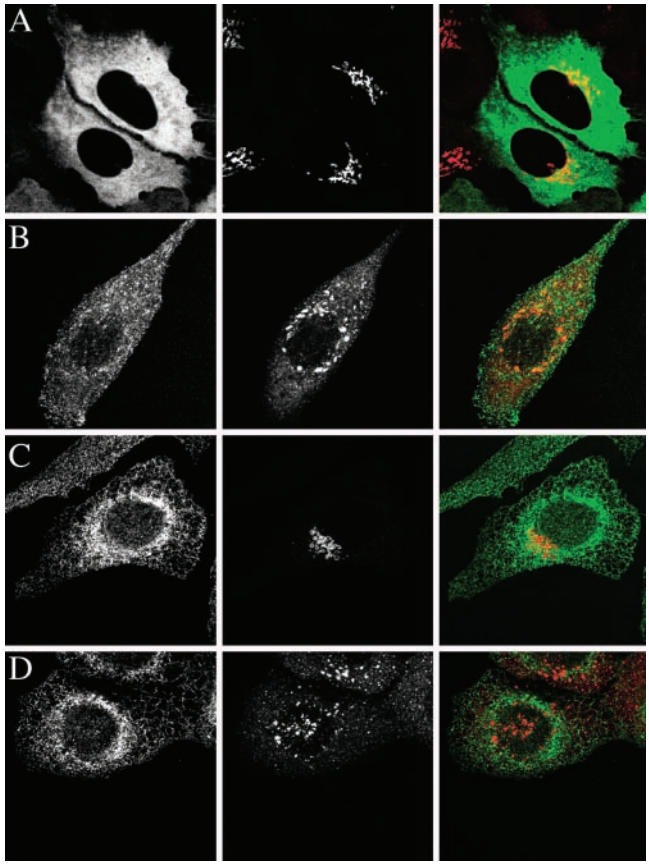

Figure 3. NSF(E329Q) disrupts the Golgi ribbon but does not affect the ER. Immunofluorescence shows (A) cytoplasmic localization of NSF-GFP (green) and normal-looking Golgi ribbons visualized with anti-giantin antibody (red), (B) punctate distribution of NSF(E329Q)-GFP (green) and disrupted Golgi membranes (anti-giantin, red). In cells expressing (C) NSF myc and (D) NSF(E329Q)myc the endoplasmic reticulum (anti-PDI, green) and Golgi apparatus (anti-giantin, red) are differentially affected. These images were collected on a confocal microscope. Each box is 83 $\times$ 83 μm.

p97(E578Q) Does Not Disrupt Golgi Structure But Causes the ER to Swell

To compare cellular activities of p97 with those of NSF, we examined the morphology of the ER and Golgi in cells expressing wtp97, p97(E305Q), or the hydrolysis-deficient p97(E578Q) mutant. This showed that expression of myc-tagged wtp97 or p97(E305Q) had no effect on either the ER (Figure 5, A and B) or the Golgi (Figure 5, E and G). Likewise, expression of p97(E578Q) had no effect on the Golgi (Figure 5, F and H) and the ER remained normal looking for several hours after induction. However, over time many cells expressing p97(E578Q) developed large vacuoles (Figure 5, C and D). These vacuoles stained in their interior with an antibody recognizing the lumenal ER protein PDI and on their limiting membrane with the ER membrane protein calnexin (Figure 5D), demonstrating that they derive from the ER. Expression of p97(E578Q) did not, however, affect distribution of the COPI coat protein β-COP (Figure 5, G vs. H) or the COPII coat component Sec23 (Figure 5, I vs. J).

Examination of p97(E578Q)-expressing cells by thin-section EM confirmed the presence of large ribosome studded vacuoles, clearly representing dilated endoplasmic reticu-

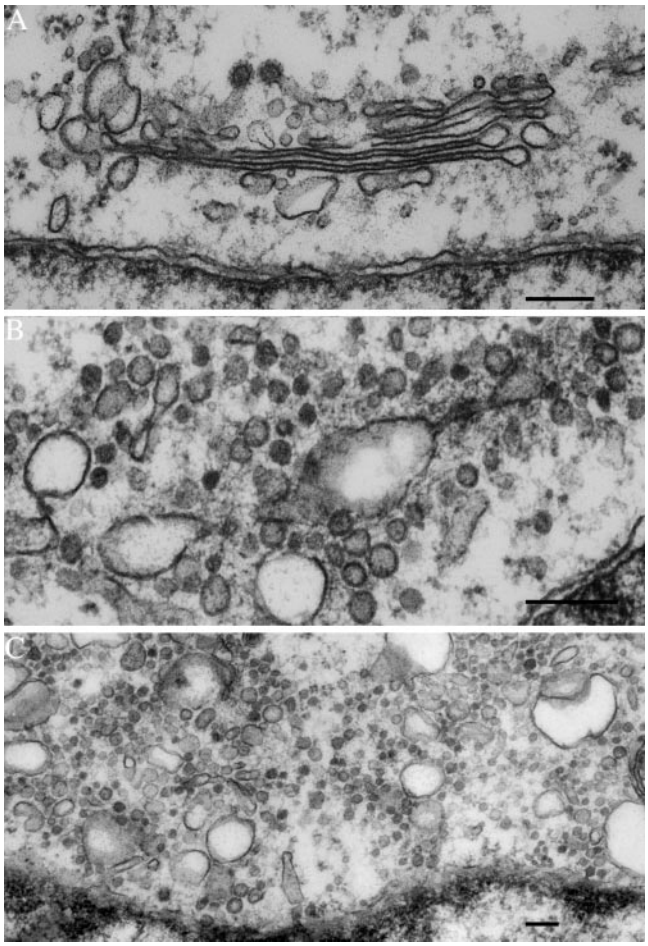

Figure 4. Ultrastructure of NSF(E329Q)-expressing cells. Thin-section EM showing normal Golgi cisternae in NSF-GFP–expressing cells (A). Similar cisternae are absent from cells expressing NSF(E329Q)-GFP. Apparent Golgi remnants (B) and pools of vesicles (C) appear adjacent to the nucleus. Scale bars, 0.2 μm.

lum (Figure 6B). In many cases, the nuclear envelope was also dilated. In contrast to normal ER (Figure 6A), the dilated ER appeared relatively devoid of stainable protein content (compare the stained material inside the ER in Figure 6A with the empty space inside the ER in Figure 6B). To more directly assess the state of organelles in p97(E578Q)-expressing cells, we quick-froze living cells and prepared them for EM by freeze-substitution (Figure 6C). The ER was still dilated and lacked content, confirming that the ER is swollen in these cells before exposure to aqueous fixatives. In contrast, the Golgi stacks in p97(E578Q) cells remained well organized (Figure 6C).

p97(E578Q) Promotes Accumulation of Ubiquitin Conjugates on the ER

What causes the ER to swell in cells expressing p97(E578Q) may have something to do with the fact that this mutant binds to ER membranes (Figures 2 and 5). An emerging theme in studies of p97 is that it participates in ubiquitin-linked protein turnover. It is involved in ERAD, wherein proteins are extracted from the ER, ubiquitinated, and then degraded by proteasomes (reviewed in Tsai *et al.,* 2002). To analyze the disposition of ubiquitinated proteins in cells expressing p97(E578Q), we used an antibody that recognizes ubiquitin conjugates (Fujimuro *et al.,* 1994; Figure 7A). This showed that expressing p97(E578Q) caused a significant build-up of ubiquitinated proteins on intracellular membranes. Importantly, p97(E578Q) itself colocalized with these ubiquitin conjugates as would be expected if it was associating directly with them. Immunoblotting confirmed that p97(E578Q) was not itself ubiquitinated (unpublished data).

The accumulation of ubiquitinated proteins on the ER in p97(E578Q)-expressing cells may reflect a defect in dislocation and subsequent degradation of membrane proteins targeted for the proteasome such as has been shown for H-2K^b in vitro (Ye *et al.,* 2001). To test this, we infected cells with adenovirus encoding the ERAD substrate ΔF508 CFTR and examined the effect of inducing either wild-type p97 or p97(E578Q) on its turnover (Figure 7B). p97(E578Q) significantly slowed degradation of ΔF508 CFTR (Figure 7B), whereas wild-type p97 did not have an effect on the turnover of ΔF508 CFTR (our unpublished observations). This confirms that ATPase activity in the D2 domain of p97 is important for efficient degradation of a known multi-transmembrane domain–containing ERAD substrate.

Effects of Inhibiting NSF and p97 on Secretory Pathway Function

The differing effects of NSF and p97 mutants on ER and Golgi structure suggest that these mutants will affect trafficking in the secretory pathway differently as well. We monitored intra-Golgi transport and secretion by measuring synthesis and release of sulfated glycosaminoglycans (GAGs; Miller and Moore, 1992; Fernandez and Warren, 1998). We found that GAG sulfation was decreased in cells expressing NSF(E329Q). Shown in Figure 8A is the inhibition in GAG synthesis seen after induction of NSF(E329Q) for different times. This time course parallels the morphological disruption of the Golgi apparatus described above and demonstrates that intra-Golgi transport is impaired by NSF(E329Q).

In contrast, GAG synthesis was not affected by expressing p97(E578Q), demonstrating that intra-Golgi transport remained normal (unpublished data). We therefore measured secretion of the sulfated GAGs to examine transport between the trans-Golgi network and the plasma membrane. Secretion was unaffected by p97(E578Q) (Figure 8B), suggesting that even when p97 activity is suppressed, the cell can transport material within its Golgi apparatus and to the cell surface.

To test the possibility that p97 might be more specifically involved in trafficking between ER and Golgi (Zhang *et al.,* 1994; Roy *et al.,* 2000), we monitored the delivery of GFP-tagged VSV-G ts045 protein from the ER to the cell surface in individual cells (Presley *et al.,* 1997). Regardless of whether p97(E578Q) was expressed or not, transferring the cells from nonpermissive to permissive temperature allowed movement of VSV-G ts045 from ER to Golgi and then to the cell surface (Figure 8C), except in cells in which the ER was fully vacuolated and thereby occupying most of the cell's volume. These experiments demonstrate that the ER remains able to concentrate and secrete cargo even when p97 activity is impaired.

Effects of p97(E578Q) on Golgi Reassembly In Vivo

Nothing in our analysis so far would suggest that p97 activity is necessary for normal function of membranes in the secretory pathway. However, because p97 has most clearly been implicated in organelle assembly reactions reconstituted in vitro (Acharya *et al.,* 1995; Latterich *et al.,* 1995; Rabouille *et al.,* 1995; Roy *et al.,* 2000; Hetzer *et al.,* 2001), we specifically asked whether p97(E578Q) expression affects de novo organelle assembly in vivo. Both p97 and NSF are

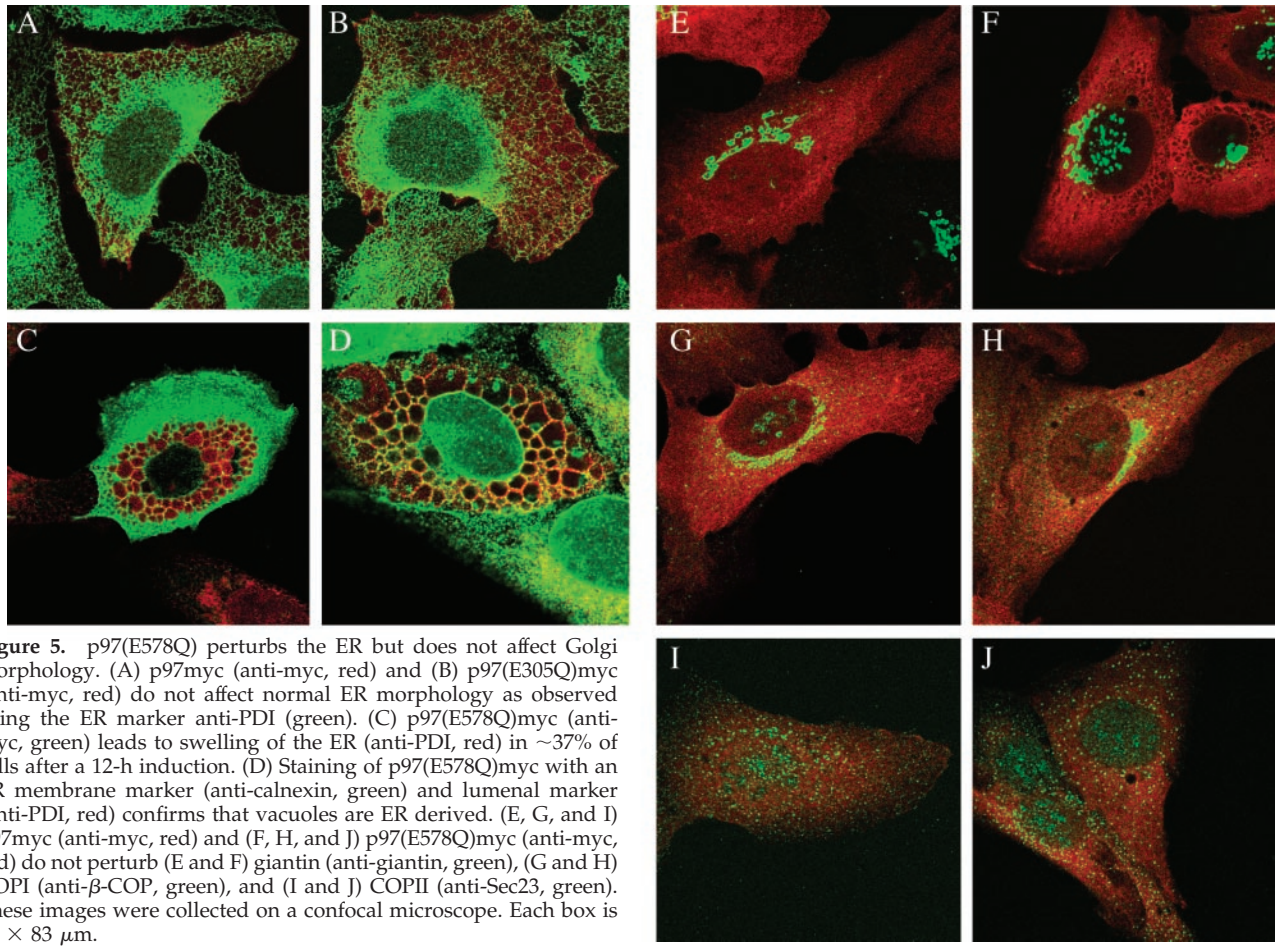

Figure 5. p97(E578Q) perturbs the ER but does not affect Golgi morphology. (A) p97myc (anti-myc, red) and (B) p97(E305Q)myc (anti-myc, red) do not affect normal ER morphology as observed using the ER marker anti-PDI (green). (C) p97(E578Q)myc (anti-myc, green) leads to swelling of the ER (anti-PDI, red) in ~37% of cells after a 12-h induction. (D) Staining of p97(E578Q)myc with an ER membrane marker (anti-calnexin, green) and lumenal marker (anti-PDI, red) confirms that vacuoles are ER derived. (E, G, and I) p97myc (anti-myc, red) and (F, H, and J) p97(E578Q)myc (anti-myc, red) do not perturb (E and F) giantin (anti-giantin, green), (G and H) COPI (anti-β-COP, green), and (I and J) COPII (anti-Sec23, green). These images were collected on a confocal microscope. Each box is 83 $\times$ 83 μm.

needed to form Golgi stacks from mitotic Golgi fragments in vitro (Rabouille *et al.*, 1995). To our surprise, p97(E578Q)-expressing cells assembled normal-looking Golgi ribbons rimmed by giantin during telophase, as assessed by light microscopy (Figure 9). Although we have not looked at these Golgi membranes by EM, we conclude from their regular organization that impairing p97 activity has little or no effect on the organization of membranes through mitosis.

A variety of pharmacologic agents also reversibly disrupt Golgi structure, including BFA, ilimaquinone, okadaic acid, and nocadozole (Dinter and Berger, 1998). We asked whether p97 is involved in Golgi reassembly after treatment with BFA. Both control U2OS and p97(E578Q)-expressing cells responded to BFA with rapid dispersal of their Golgi membranes (Figure 10). Removing BFA from these cells led to the prompt reformation of normal-looking Golgi apparati even in cells whose ER had visibly swollen. Hence, assembly of Golgi ribbons after mitotic or chemical dispersion does not appear, in our in vivo studies, to require p97's ATPase activity.

DISCUSSION

In this study, we have used dominant interfering mutants to define the roles that the AAA ATPases NSF and p97 play in the structure and function of the secretory pathway in animal cells. We confirm that NSF's ATPase activity is essential for transport through the Golgi apparatus and show that interfering with this activity promotes disassembly of Golgi stacks. Surprising in comparison is the finding that inhibit-

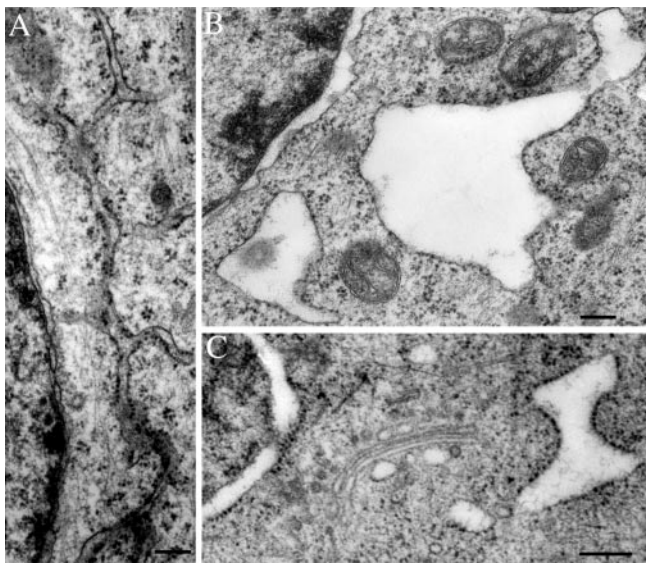

Figure 6. Dilated ER and nuclear envelope in p97(E578Q) expressing cells. Traditional thin section EM of (A) a p97(E578Q)myc expressing cell in which the ER looks relatively normal, (B) a p97(E578Q)myc expressing cell containing swollen ribosome-studded ER. (C) Thin-section EM of freeze substituted p97(E578Q)myc-expressing cell showing swollen ER and nuclear envelope together with apparently normal Golgi. Scale bars, 0.2 μm.

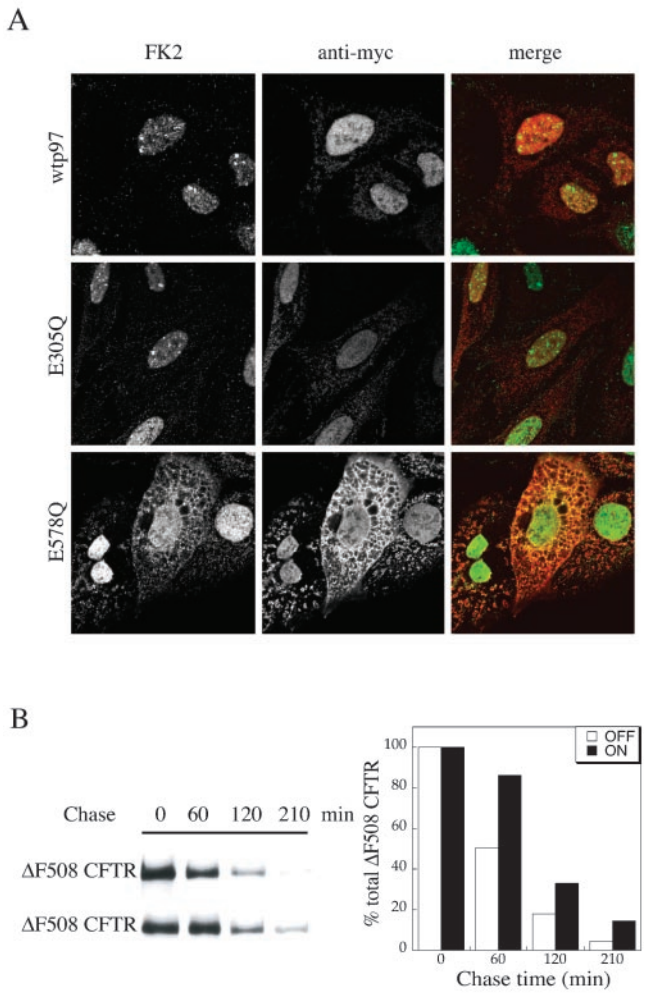

Figure 7. p97(E578Q) causes accumulation of ubiquitinated proteins on ER membranes and a delay in ΔF508 CFTR degradation. (A) After saponin permeabilization, retained ubiquitin-conjugates (FK2, green), and p97myc, p97(E305Q)myc, or p97(E578Q)myc (anti-myc, red) were visualized by immunofluorescence. These images were collected on a confocal microscope. Each box is 73 × 73 μm. (B) Pulse chase analysis of ΔF508 CFTR turnover in cells expressing (ON) or not (OFF) p97(E578Q). Immunoprecipitated ΔF508 CFTR is shown in the autoradiographs on the left (OFF, top; ON, bottom), and quantitated by densitometry on the right. The data presented are representative of four independent trials.

ing p97 does not affect membrane trafficking. The Golgi apparatus remains intact and secretion is unimpaired, despite accumulation of ubiquitinated proteins on the ER. The nonoverlapping effects of inhibiting these two AAA ATPases in vivo suggest that NSF and p97 have primary roles in different cellular reactions.

NSF and Membrane Fusion

Many experiments have shown that NSF is essential for proper assembly and function of organelles in the secretory and endocytic pathways (reviewed in Whiteheart *et al.*, 2001). NSF operates in these reactions at least in part by dissociating SNARE complexes that form during membrane fusion (Söllner *et al.*, 1993). Thus, we expected that inhibiting NSF activity by expressing a dominant interfering mutant would impair movement between intracellular compartments and disrupt the organization of the secretory pathway. This was indeed the case. The ultrastructural appearance of membranes in NSF(E329Q)-expressing cells (Figure 4) recapitulates the accumulation of vesicles seen after NEM treatment of Golgi membranes in vitro as well as after treatment of whole cells with NEM (Orci *et al.*, 1989). Interestingly, Golgi membranes dispersed by NSF(E329Q) (Figure 3) did not appear to fuse with the ER, but instead moved around the cell and ended up clustered near the nucleus (our unpublished observations). A likely explanation for the lack of fusion between these Golgi-derived vesicles and the ER is that they contain inappropriate *cis*-SNARE complexes that cannot participate in fusion. Such an accumulation of SNARE complexes has been shown to happen after inactivating NSF in *Drosophila* (Littleton *et al.*, 1998; Tolar and Pallanck, 1998; Mohtashami *et al.*, 2001) and yeast (Grote *et al.*, 2000).

The affinity of AAA proteins for substrates is typically highest in the ATP-bound state (Hanson *et al.*, 1997; Vale, 2000); hence the localization of hydrolysis deficient (presumably ATP-bound) NSF(E329Q) should reflect the distribution of NSF's substrates in the cell. In fact, this mutant was almost completely retained on membranes (Figure 2). Although we could not identify all of the membranes that recruited NSF(E329Q), many contained markers for the Golgi apparatus (Figure 3) or the late endosome (LAMP2, our unpublished observations). Consistent with this recruitment to endosomal membranes, NSF(E329Q) has previously been shown to interfere with phagocytosis and endosomal maturation (Coppolino *et al.*, 2001). Golgi and endosome membranes are among the most dynamic in the cell and thus are likely to have the highest concentration of SNAREs to recruit NSF. ER membranes in contrast recruited little NSF(E329Q), despite the known ability of their SNAREs to bind α-SNAP and NSF (Hay *et al.*, 1997; Hatsuzawa *et al.*, 2000), indicating that they may have a low concentration of SNAREs.

p97 Function in U2OS Cells

p97 (Cdc48p in yeast) has been implicated in membrane fusion based on its role in assays that reconstitute aspects of organelle assembly in vitro (see Introduction and below). We therefore expected that inhibiting p97 in vivo would at least partially disrupt ER and Golgi structure and function. When this did not happen (Figures 5 and 8), we looked specifically at Golgi reassembly under circumstances similar to those in which p97 had been studied in vitro (Acharya *et al.*, 1995; Rabouille *et al.*, 1995). Hydrolysis-deficient p97 did not block the cells' ability to progress into and through mitosis, allowing successful reassembly of Golgi apparati during telophase (Figure 9). Similarly, mutant p97 did not interfere with BFA-induced disassembly or postwashout recovery of the Golgi ribbon (Figure 10).

However, before concluding from these results that p97 is not directly involved in the membrane fusion needed to assemble and restructure the Golgi, we had to be sure that expressing p97(E578Q) inhibited some known function of p97. Indeed, cells induced for p97(E578Q) accumulated ubiquitin-conjugated proteins on their ER (Figure 7). p97 is known to participate in the dislocation of membrane proteins destined for degradation by ERAD (Tsai *et al.*, 2002; Ye *et al.*, 2003), and one predicted effect of inhibiting its activity in ERAD would be just such an accumulation of ubiquitinated proteins. In a more direct assessment of how inhibiting p97 affects ERAD, we found that expressing p97(E578Q) in our cells slows degradation of the known ERAD substrate ΔF508 CFTR (Figure 7). Accumulation of ΔF508 CFTR in

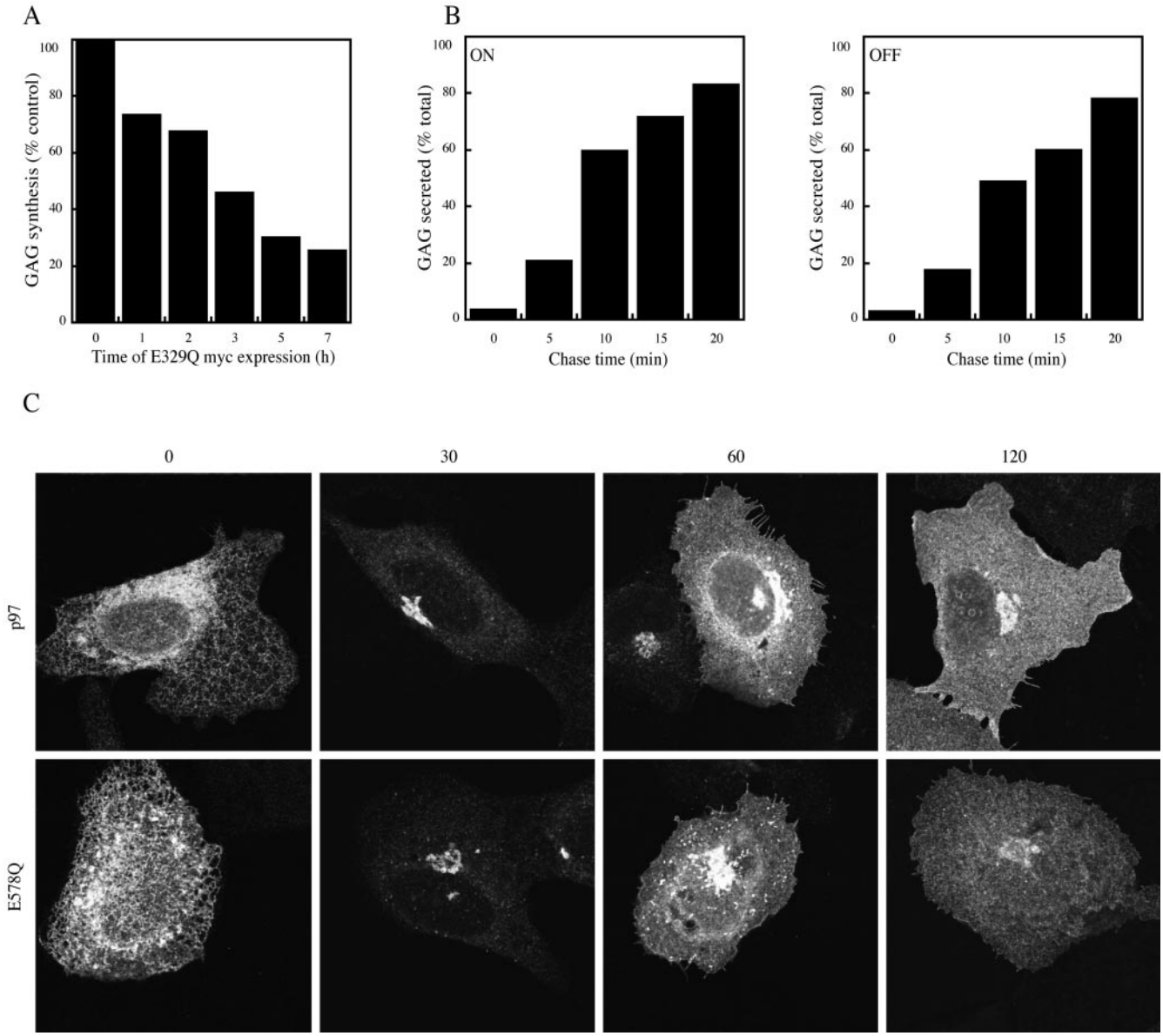

Figure 8. NSF(E329Q) disrupts Golgi function, whereas p97(E578Q) does not. (A) Synthesis of ^{35}S-sulfated GAGs as a function of the time of NSF(E329Q)myc induction. Data for the different time points were normalized relative to 100% for the 0 time point. (B) Secretion of ^{35}S-sulfated GAGs relative to the total ^{35}S-sulfated GAGs synthesized for different chase times in p97(E578Q)myc cells that were induced for 12 h (ON) or were not induced (OFF). (C) VSV-G ts045-GFP distribution in p97myc cells (top panel) and p97(E578Q)myc cells induced for 12 h (bottom panel) at 0, 30, 60, and 120 min after shifting the cells from the nonpermissive temperature (38.5°C) to the permissive temperature (32°C). These images were obtained on a confocal microscope. Each box is 92 × 92 μm.

cells overexpressing a p97 Walker A motif mutant has also recently been reported (Kobayashi *et al.*, 2002). Additional evidence that p97(E578Q) interferes with p97's normal activity came from finding that it causes the ER to vacuolate.

Although the secretory pathway remained functional, expressing p97(E578Q) did lead to dramatic dilation of the ER (Figures 5 and 6; see also Hirabayashi *et al.*, 2001; Kobayashi *et al.*, 2002). Why the ER swells after inhibiting p97 is not clear, but may be related to the activity associated with one of its cofactors, SVIP, because manipulating SVIP causes a similar dilation of the ER (Nagahama *et al.*, 2003). These morphological changes seem unlikely to be caused by a defect in membrane fusion between tubules of the ER. The predicted outcome of such a block in fusion would be an ER network with a lower than normal number of 3-way junctions and not the dilated ER that we observed. One possibility is that the ER dilates because of the impairment in ERAD or related degradative processes (Figure 7). This is suggested by the fact that similar swelling can be induced by treating cells with the proteasome inhibitors PSI and MG115 and antagonized by overexpressing wild-type p97 (Hirabayashi *et al.*, 2001). We do not, however, think that ER dilation is the result of global accumulation of misfolded proteins in the ER lumen because adding cycloheximide after a short induction of p97(E578Q) did not prevent it (our unpublished observations). Another possible explanation for the swelling would be a change in the organization of ER subdomains. Such disorganization could result in changes in the ratio,

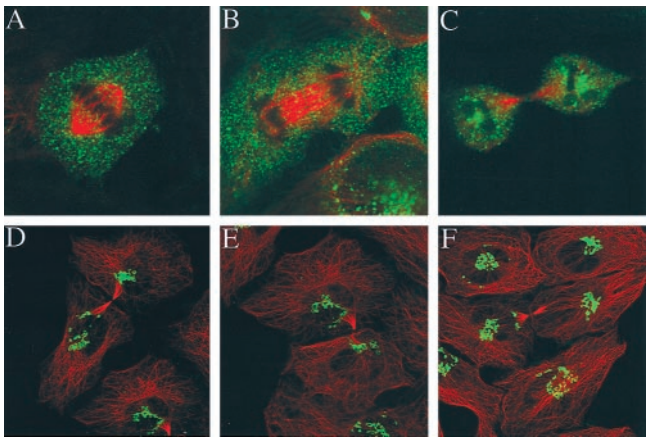

Figure 9. p97(E578Q) does not affect Golgi distribution mitosis. p97(E578Q)myc cells at different stages of mitosis stained with anti-giantin (green) and anti-α-tubulin (red). (A) metaphase, (B) anaphase, (C) telophase I, (D–F) telophase II. Images were obtained on a confocal microscope. (A–C) Each box is 40 × 40 μm. (D–F) Each box is 83 × 83 μm.

size, and shape of ER cisternae and tubules. Morphologically similar swelling is seen in a few pathological conditions, including intoxication with the pore forming toxin aerolysin (Abrami *et al.*, 1998), prolonged exposure of cells to BFA (Alvarez and Sztul, 1999), and treatment of neurons with tunicamycin (Lin *et al.*, 1999). Further understanding of the events that lead to ER dilation will shed light on how p97 participates in ER homeostasis.

The apparent absence of an obligate role for p97 in membrane trafficking is, in fact, consistent with a number of previous studies. For one, conditional mutants in Cdc48p do not have a secretion defect. *Cdc48* mutants are unable to divide their nuclei during cell division and unable to fuse their nuclei during karyogamy (Moir *et al.*, 1982; Fröhlich *et al.*, 1991; Latterich *et al.*, 1995). Despite the fact that ER

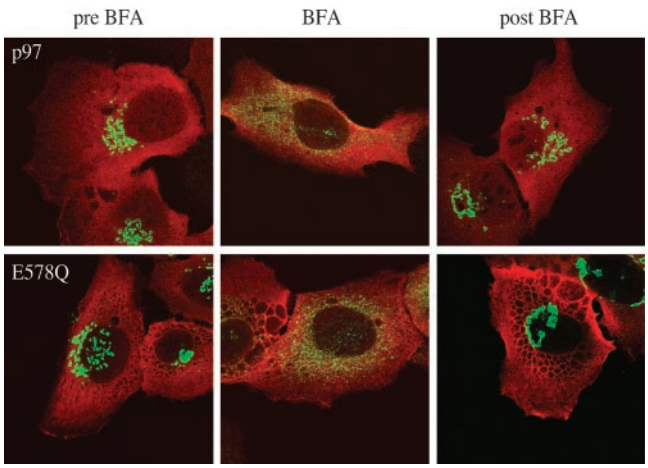

Figure 10. Disruption and reassembly of Golgi ribbon in response to BFA are unaffected by p97(E578Q). p97myc cells (top panel) and p97(E578Q)myc cells (bottom panel) are shown from left to right before BFA addition, after BFA treatment for 40 min, and after recovery from BFA for 120 min, respectively. Giantin is in green (anti-giantin) and p97(E578Q)myc is in red (anti-myc). Images were obtained on a confocal microscope. Each box is 83 × 83 μm.

membranes from *cdc48* mutant yeast are defective in fusion in vitro (Latterich *et al.*, 1995), the peripheral ER in such cells behaves normally (and dynamically) in vivo, even at temperatures nonpermissive for Cdc48p function (Prinz *et al.*, 2000). This suggests that Cdc48p operates on membranes only under specialized conditions. In mammalian systems, p97 plays some role in the in vitro assays described in the Introduction and below, but is not required for intercompartmental Golgi transport between Golgi stacks (Fernandez and Warren, 1998).

p97 and Membrane Fusion

How do we reconcile the seeming disparity between previous studies that describe a need for p97 in specialized membrane fusion reactions and our finding that dominant interfering mutants do not readily disrupt membrane trafficking or organelle structure in vivo? Formal possibilities include 1) the small proportion of unpoisoned endogenous p97 hexamer remaining after induction of p97(E578Q) can support membrane fusion but not ubiquitin related processes, 2) membrane fusion but not ubiquitin related processes can persist in the presence of mixed hexamers containing endogenous and p97(E578Q) subunits, and 3) membrane fusion can selectively proceed in the absence of ATPase activity. However, we think these explanations are rather unlikely. Most endogenous p97 subunits coassemble with p97(E578Q) subunits. Moreover, even if endogenous holoenzymes remain, they would be unlikely to function normally because of the persistent interaction between mutant p97 and substrates.

To reconcile our results with previous studies, we first review the evidence that implicates p97 in membrane fusion. p97 participates in reassembly of ilimaquinone dispersed Golgi membranes into Golgi stacks (Acharya *et al.*, 1995), reformation of unfenestrated Golgi cisternae from mitotic Golgi fragments (Rabouille *et al.*, 1995, 1998), fusion of yeast ER membranes (Latterich *et al.*, 1995; Lin *et al.*, 2001), formation but not maintenance of tubulated ER from low-density microsomes (Lavoie *et al.*, 2000; Roy *et al.*, 2000), and formation and growth of the nuclear envelope and associated ER network (Hetzer *et al.*, 2001). These in vitro assays all reconstitute complex processes related to organelle assembly. The membranes involved must undergo not only fusion but also profound shape changes to generate the structures that are the end points of the assays. These systems have led to discovery of proteins that directly participate in membrane fusion, but it may be difficult to distinguish between such proteins and others that are less directly involved.

More recently, Kondo and coworkers have shown that the p97 adapter proteins p47 and VCIP135 are required in vivo for reassembly of the Golgi apparatus and formation of the ER network upon exit from mitosis (Uchiyama *et al.*, 2002, Uchiyama *et al.*, 2003). Although these studies may point to a specific role for p97 in membrane fusion, both adaptor proteins are also directly linked to ubiquitin pathways. p47 and VCIP135 each contain a ubiquitin-like domain, and p47 also contains a ubiquitin binding domain (Meyer *et al.*, 2002; Uchiyama *et al.*, 2002). Perturbations in ubiquitin homeostasis caused by interfering with these proteins during cell division may complicate analysis of p97's function in postmitotic organelle assembly.

All of the above studies taken together have led to the current model that p97 participates in both membrane fusion and protein degradation via interaction with distinct adaptor proteins (Meyer *et al.*, 2002). The direct inhibition of p97 reported in this study (without changes in the adaptor proteins) suggests that p97's central function in the cell is in

controlling ubiquitin-dependent processes. Although this places p97 in a position to regulate a large number of cellular events, we do not see evidence for an obvious role in membrane fusion. This is in contrast to NSF, for which our experiments point convincingly to a primary and essential role in membrane fusion. We propose that p97's normal role—if any—in controlling membrane fusion is therefore likely to be different from that of NSF. An interesting possibility is that p97-controlled protein degradation could regulate ER, nuclear envelope, and Golgi assembly.

ACKNOWLEDGMENTS

We thank John Heuser for generously sharing his expertise in microscopy, useful discussions, and a critical review of the manuscript. We thank Robyn Roth and Marilyn Levy for excellent assistance with EM sample preparation and imaging. We are also grateful to Adam Linstedt for providing the VSV-G ts045 GFP construct, Wally Whiteheart for the mouse p97 DNA construct, Reinhard Jahn for antibodies against NSF and α-SNAP, and Graham Warren for antibody against p47. We thank members of the Hanson lab for useful discussions and technical assistance; Mike Green, Peggy Weidman, and Vivek Malhotra for helpful suggestions; and Paul Nghiem for advice on U2OS cells. This work was supported by Grant NS38058 from the National Institutes of Health, W.M. Keck Foundation Distinguished Scholar and Searle Scholar Awards to P.I.H., and an NRSA postdoctoral fellowship (NS41709) to S.D.

REFERENCES

Abrami, L., Fivaz, M., Glauser, P., Parton, R., and van der Goot, F. (1998). A pore-forming toxin interacts with a GPI-anchored protein and causes vacuolation of the endoplasmic reticulum. J. Cell Biol. *140,* 525–540.

Acharya, U., Jacobs, R., Peters, J., Watson, N., Farquhar, M., and Malhotra, V. (1995). The formation of Golgi stacks from vesiculated Golgi membranes requires two distinct fusion events. Cell *82,* 895–904.

Alvarez, C., and Sztul, E. (1999). Brefeldin A (BFA) disrupts the organization of the microtubule and actin cytoskeletons. Eur. J. Cell Biol. *78,* 1–14.

Bays, N., and Hampton, R. (2002). Cdc48–Ufd1–Npl *4,* stuck in the middle with Ub. Curr. Biol. *12,* R366–R371.

Coppolino, M.G., Kong, C., Mohtashami, M., Schreiber, A.D., Brumell, J.H., Finlay, B.B., Grinstein, S., Trimble, W.S. (2001). Requirement for *N*-ethylmaleimide-sensitive factor activity at different stages of bacterial invasion and phagocytosis. J. Biol. Chem. *276,* 4772–4780.

Beuron, F., Flynn, T.C., Ma, J., Kondo, H., Zhang, X., and Freemont, P.S. (2003). Motions and negative cooperativity between p97 domains revealed by cryo-electron microscopy and quantised elastic deformational model. J. Mol. Biol. *327,* 619–629.

Dai, R., Chen, E., Longo, D., Gorbea, C., and Li, C. (1998). Involvement of valosin-containing protein, an ATPase co-purified with IκBα and 26S proteasome, in ubiquitin-proteasome-mediated degradation of IκBα. J. Biol. Chem. *273,* 3562–3573.

Dai, R., and Li, C. (2001). Valosin-containing protein is a multi-ubiquitin chain-targeting factor required in ubiquitin-proteasome degradation. Nat. Cell Biol. *3,* 740–744.

DeLaBarre, B., and Brünger, A.T. (2003). Complete structure of p97/valosin-containing protein reveals communication between nucleotide domains. Nat. Struct. Biol. *10,* 856–863.

Dinter, A., and Berger, E. (1998). Golgi-disturbing agents. Histochem. Cell Biol. *109,* 571–590.

Egerton, M., and Samelson, L.E. (1994). Biochemical characterization of valosin-containing protein, a protein tyrosine kinase substrate in hematopoietic cells. J. Biol. Chem. *269,* 11435–11441.

Fernandez, C., and Warren, G. (1998). In vitro synthesis of sulfated glycosaminoglycans coupled to inter-compartmental Golgi transport. J. Biol. Chem. *273,* 19030–19039.

Fröhlich, K., Fries, H., Rudiger, M., Erdmann, R., Botstein, D., and Mecke, D. (1991). Yeast cell cycle protein CDC48p shows full-length homology to the mammalian protein VCP and is a member of a protein family involved in secretion, peroxisome formation, and gene expression. J. Cell Biol. *114,* 443–453.

Fujimuro, M., Sawada, H., and Yokosawa, H. (1994). Production and characterization of monoclonal antibodies specific to multi-ubiquitin chains of polyubiquitinated proteins. FEBS Lett. *349,* 173–180.

Ghislain, M., Dohmen, R., Levy, F., and Varshavsky, A. (1996). Cdc48p interacts with Ufd3p, a WD repeat protein required for ubiquitin-mediated proteolysis in Saccharomyces cerevisiae. EMBO J. *15,* 4884–4899.

Goda, Y., and Pfeffer, S.R. (1991). Identification of a novel, *N*-ethylmaleimide-sensitive cytosolic factor required for vesicular transport from endosomes to the trans-Golgi network in vitro. J. Cell Biol. *112,* 823–831.

Grote, E., Carr, C.M., and Novick, P.J. (2000). Ordering the final events in yeast exocytosis. J. Cell Biol. *16,* 439–452.

Hanson, P., Roth, R., Morisaki, H., Jahn, R., and Heuser, J. (1997). Structure and conformational changes in NSF and its membrane receptor complexes visualized by quick-freeze/deep-etch electron microscopy. Cell *90,* 523–535.

Hay, J.C., Chao, D.S., Kuo, C.S., and Scheller, R.H. (1997). Protein interactions regulating vesicle transport between the endoplasmic reticulum and Golgi apparatus in mammalian cells. Cell *89,* 149–58.

Hatsuzawa, K., Hirose, H., Tani, K., Yamamoto, A., Scheller, R.H., and Tagaya, M. (2000). Syntaxin 18, a SNAP receptor that functions in the endoplasmic reticulum, intermediate compartment, and cis-Golgi vesicle trafficking. J. Biol. Chem. *275,* 13713–13720.

Hetzer, M., Meyer, H., Walther, T., Bilbao-Cortes, D., Warren, G., and Mattaj, I. (2001). Distinct AAA-ATPase p97 complexes function in discrete steps of nuclear assembly. Nat. Cell Biol. *3,* 1086–1091.

Heuser, J.E., and Reese, T.S. (1981). Structural changes after transmitter release at the frog neuromuscular junction. J. Cell Biol. *88,* 564–580.

Heuser, J.E., Reese, T.S., Dennis, M.J., Jan, Y., Jan, L., and Evans, L. (1979). Synaptic vesicle exocytosis captured by quick freezing and correlated with quantal transmitter release. J. Cell Biol. *81,* 275–300.

Hirabayashi, M. *et al.* (2001). VCP/p97 in abnormal protein aggregates, cytoplasmic vacuoles, and cell death, phenotypes relevant to neurodegeneration. Cell Death Differ. *8,* 977–984.

Hung, L.W., Wang, I.X., Nikaido, K., Liu, P.Q., Ames, G.F., and Kim, S.H. (1998). Crystal structure of the ATP-binding subunit of an ABC transporter. Nature *396,* 703–707.

Jahn, R., Lang, T., and Südhof, T.C. (2003). Membrane fusion. Cell *112,* 519–533.

Kobayashi, T., Tanaka, K., Inoue, K., and Kakizuka, A. (2002). Functional ATPase activity of p97/valosin-containing protein (VCP) is required for the quality control of endoplasmic reticulum in neuronally differentiated mammalian PC12 cells. J. Biol. Chem. *277,* 47358–47365.

Kondo, H., Rabouille, C., Newman, R., Levine, T., Pappin, D., Freemont, P., and Warren, G. (1997). p47 is a cofactor for p97-mediated membrane fusion. Nature *388,* 75–78.

Lamb, J., Fu, V., Wirtz, E., and Bangs, J. (2001). Functional analysis of the trypanosomal AAA protein TbVCP with transdominant ATP hydrolysis mutants. J. Biol. Chem. *276,* 21512–21520.

Latterich, M., Frohlich, K.-U., and Schekman, R. (1995). Membrane fusion and the cell cycle: Cdc48p participates in the fusion of ER membranes. Cell *82,* 885–893.

Latterich, M., and Schekman, R. (1994). The karyogamy gene KAR2 and novel proteins are required for ER-membrane fusion. Cell *78,* 87–98.

Lavoie, C., Chevet, E., Roy, L., Tonks, N.K., Fazel, A., Posner, B.I., Paiement, J., and Bergeron, J.J. (2000). Tyrosine phosphorylation of p97 regulates transitional endoplasmic reticulum assembly in vitro. Proc. Natl. Acad. Sci. USA *97,* 513637–513642.

Lill, R., Dowhan, W., and Wickner, W. (1990). The ATPase activity of SecA is regulated by acid phospholipids, SecY, and the leader and mature domains of precursor proteins. Cell *60,* 271–280.

Lin, T-Y., Wang, S-M., Fu, W-M., Chen, Y-H., and Yin, H-S. (1999). Toxicity of tunicamycin to cultured brain neurons: ultrastructure of the degenerating neurons. J. Cell. Biochem. *74,* 638–647.

Lin, A., Patel, S., and Latterich, M. (2001). Regulation of organelle membrane fusion by Pkc1p. Traffic *2,* 698–704.

Littleton, J., Chapman, E., Kreber, R., Garment, M., Carlson, S., and Ganetzky, B. (1998). Temperature-sensitive paralytic mutations demonstrate that synaptic exocytosis requires SNARE complex assembly and disassembly. Neuron *21,* 401–413.

Meacham, G.C., Lu, Z., King, S., Sorscher, E., Tousson, A., and Cyr, D.M. (1999). The Hdj-2/Hsc70 chaperone pair facilitates early steps in CFTR biogenesis. EMBO J. *18,* 1492–1505.

Meyer, H., Kondo, H., and Warren, G. (1998). The p47 co-factor regulates the ATPase activity of the membrane fusion protein, p97. FEBS Lett. *437,* 255–257.

Meyer, H., Shorter, J., Seeman, J., Pappin, D., and Warren, G. (2000). A complex of mammalin ufd1 and npl4 links the AAA-ATPase, p97, to ubiquitin and nuclear transport pathways. EMBO J. *19,* 2181–2192.

Meyer, H., Wang, Y., and Warren, G. (2002). Direct binding of ubiquitin conjugates by the mammalian p97 adaptor complexes, p47 and Ufd1-Npl4. EMBO J. *21,* 5645–5652.

Miller, S., and Moore, H. (1992). Movement from trans-Golgi network to cell surface in semiintact cells. Methods Enzymol. *219,* 234–248.

Mohtashami, M., Stewart, B.A., Boulianne, G.L., and Trimble, W.S. (2001). Analysis of the mutant Drosophila *N*-ethylmaleimide sensitive fusion-1 protein in comatose reveals molecular correlates of the behavioural paralysis. J. Neurochem. *77,* 1407–1417.

Moir, D., Stewart, S., Osmond, B., and Botstein, D. (1982). Cold-sensitive cell-division-cycle mutants of yeast: isolation, properties, and pseudoreversion studies. Genetics *100,* 565–577.

Nagahama, M., Suzuki, M., Hamada, Y., Hatsuzawa, K., Tani, K., Yamamoto, A., and Tagaya, M. (2003). SVIP is a novel VCP/p97-interacting protein whose expression causes cell vacuolation. Mol. Biol. Cell *14,* 262–273.

Nagiec, E.E., Bernstein, A., and Whiteheart, S.W. (1995). Each domain of the N-ethylmaleimide-sensitive fusion protein contributes to its transport activity. J. Biol. Chem. *270,* 29182–29188.

Neuwald, A., Aravind, L., Spouge, J., and Koonin, E. (1999). AAA^{+}: a class of chaperone-like ATPases associated with the assembly, operation, and disassembly of protein complexes. Genome Res. *9,* 27–43.

Orci, L., Malhotra, V., Amherdt, M., Serafini, T., and Rothman, J. (1989). Dissection of a single round of vesicular transport: sequential intermediates for intercisternal movement in the Golgi stack. Cell *56,* 357–368.

Patel, S.K., Indig, F.E., Olivieri, N., Levine, N.D., and Latterich, M. (1998). Organelle membrane fusion: a novel function for the syntaxin homolog Ufe1p in ER membrane fusion. Cell *92,* 611–620.

Peters, J.-M., Harris, J.R., Lustig, A., Muller, S., Engel, A., Volker, S., and Franke, W.W. (1992). Ubiquitous soluble Mg^{2+}-ATPase complex. A structural study. J. Mol. Biol. *223,* 557–571.

Peters, J.-M., Walsh, M.J., and Franke, W.W. (1990). An abundant and ubiquitous homo-oligomeric ring-shaped ATPase particle related to the putative vesicle fusion proteins Sec18p and NSF. EMBO J. *9,* 1757–1767.

Presley, J., Cole, N., Schroer, T., Hirschberg, K., Zaal, K., and Lippincott-Schwartz, J. (1997). ER-to-Golgi transport visualized in living cells. Nature *389,* 81–85.

Prinz, W., Grzyb, L., Veenhuis, M., Kahana, J., Silver, P., and Rapoport, T. (2000). Mutants affecting the structure of the cortical endoplasmic reticulum in Saccharomyces cerevisiae. J. Cell Biol. *150,* 461–474.

Rabouille, C., Kondo, H., Newman, R., Hui, N., Freemont, P., and Warren, G. (1998). Syntaxin 5 is a common component of the NSF- and p97-mediated reassembly pathways of Golgi cisternae from mitotic Golgi fragments in vitro. Cell *92,* 603–610.

Rabouille, C., LeVine, T.P., Peters, J.-M., and Warren, G. (1995). An NSF-like ATPase, p97, and NSF mediate cisternal regrowth from mitotic Golgi fragments. Cell *82,* 905–914.

Rape, M., Hoppe, T., Gorr, I., Kalocay, M., Richly, H., and Jentsch, S. (2001). Mobilization of processed, membrane-tethered SPT23 transcription factor by CDC48(UFD1/NPL4), a ubiquitin-selective chaperone. Cell *107,* 667–677.

Rodriguez, L., Stirling, C.J., and Woodman, P.G. (1994). Multiple N-ethylmaleimide-sensitive components are required for endosomal vesicle fusion. Mol. Biol. Cell *5,* 773–783.

Rouiller, I., DeLaBarre, B., May, A., Weis, W., Brünger, A., Milligan, R., and Wilson-Kubalek, E. (2002). Conformational changes of the multifunctional p97 AAA ATPase during its ATPase cycle. Nat. Struct. Biol. *9,* 950–957.

Rouiller, I., Butel, V.M., Latterich, M., Milligan, R.A., and Wilson-Kubalek, E.M. (2000). A major conformational change in p97 AAA ATPase upon ATP binding. Mol. Cell *6,* 1485–1490.

Roy, L., Bergeron, J.J., Lavoie, C., Hendriks, R., Gushue, J., Fazel, A., Pelletier, A., Morre, D.J., Subramaniam, V.N., Hong, W., and Paiement, J. (2000). Role of p97 and syntaxin 5 in the assembly of transitional endoplasmic reticulum. Mol. Biol. Cell *11,* 2529–2542.

Song, C., Wang, Q., and Li, C. (2003). ATPase activity of p97-VCP. D2 mediates the major enzyme activity, and D1 contributes to the heat induced activity. J. Biol. Chem. *278,* 3648–3655.

Söllner, T., Bennett, M.K., Whiteheart, S.W., Scheller, R.H., and Rothman, J.E. (1993). A protein assembly-disassembly pathway in vitro that may correspond to sequential steps of synaptic vesicle docking, activation, and fusion. Cell *75,* 409–418.

Tolar, L.A., and Pallanck, L. (1998). NSF function in neurotransmitter release involves rearrangement of the SNARE complex downstream of synaptic vesicle docking. J. Neurosci. *18,* 10250–10256.

Tsai, B., Ye, Y., and Rapoport, T. (2002). Retro-translocation of proteins from the endoplasmic reticulum into the cytosol. Nat. Rev. Mol. Cell. Biol. *3,* 246–255.

Uchiyama, K., Jokitalo, E., Lindman, M., Jackman, M., Kano, F., Murata, M., Zhang, X., and Kondo, H. (2003). The localization and phosphorylation of p47 are important for Golgi disassembly-assembly during the cell cycle. J. Cell Biol. *161,* 1067–1079.

Uchiyama, K., Jokitalo, E., Kano, F., Murata, M., Zhang, X., Canas, B., Newman, R., Rabouille, C., Pappin, D., Freemont, P., Kondo, H. (2002). VCIP135, a novel essential factor for p97/p47-mediated membrane fusion, is required for Golgi and ER assembly in vivo. J. Cell Biol. *159,* 855–866.

Vale, R. (2000). AAA proteins. Lords of the ring. J. Cell Biol. *150,* F13–F20.

Wang, Q., Song, C., and Li, C.C. (2003). Hexamerization of p97-VCP is promoted by ATP binding to the D1 domain and required for ATPase and biological activities. Biochem. Biophys. Res. Commun. *300,* 253–260.

Whiteheart, S., Schraw, T., and Matveeva, E. (2001). *N*-ethylmaleimide sensitive factor (NSF) structure and function. Int. Rev. Cytol. *207,* 71–112.

Whiteheart, S.W., Rossnagel, K., Buhrow, S.A., Brunner, M., Jaenicke, R., and Rothman, J.E. (1994). *N*-ethylmaleimide-sensitive fusion protein: a trimeric ATPase whose hydrolysis of ATP is required for membrane fusion. J. Cell Biol. *126,* 945–954.

Wilson, D.W., Wilcox, C.A., Flynn, G.C., Chen, E., Kuang, W.J., Henzel, W.J., Block, M.R., Ullrich, A., and Rothman, J.E. (1989). A fusion protein required for vesicle-mediated transport in both mammalian cells and yeast. Nature *339,* 355–359.

Wilson, K.L. (1995). NSF-independent fusion mechanisms. Cell *81,* 475–477.

Ye, Y., Meyer, H.H., and Rapoport, T.A. (2001). The AAA ATPase Cdc48/p97 and its partners transport proteins from the ER into the cytosol. Nature *414,* 652–656.

Ye, Y., Meyer, H.H., and Rapoport, T.A. (2003). Function of the p97-Ufd1-Npl4 complex in retrotranslocation from the ER to the cytosol: dual recognition of nonubiquitinated polypeptide segments and polyubiquitin chains. J. Cell Biol. *7,* 71–84.

Yuan, X., Shaw, A., Zhang, X., Kondo, H., Lally, J., Freemont, P., and Matthews, S. (2001). Solution structure and interaction surface of the C-terminal domain from p *47,* a major p97-cofactor involved in SNARE disassembly. J. Mol. Biol. *311,* 255–263.

Zhang, L., Ashendel, C.L., Becker, G.W., and Morre, D.J. (1994). Isolation and characterization of the principal ATPase associated with transitional endoplasmic reticulum of rat liver. J. Cell Biol. *127,* 1871–1883.